This is a post-peer-review, pre-copyedit version of an article published in Bulletin of Earthquake Engineering. The final authenticated version is available online at: http://dx.doi.org/10.1007/s10518-019-00669-2

VALIDATION AND EXTENSION OF A STATISTICAL USABILITY MODEL FOR UNREINFORCED MASONRY BUILDINGS WITH DIFFERENT GROUND MOTION INTENSITY MEASURES

Maria Zucconi[1], Rachele Ferlito[2], Luigi Sorrentino[3]

[1] Department of Engineering, University Niccolò Cusano, Via Don Carlo Gnocchi 3, 00166 Roma, Italy, maria.zucconi@unicusano.it, corresponding author

[2] Seismic and Volcanic Risk Office, Civil Protection Department, Via Vitorchiano 4, 00189 Roma, Italy, rachele.ferlito@protezionecivile.it

[3] Department of Structural and Geotechnical Engineering, Sapienza – University of Rome, Via Antonio Gramsci 53, 00197 Roma, Italy, luigi.sorrentino@uniroma1.it

ABSTRACT

Predicting the usability of a building, i.e. its condition of being occupiable after a seismic event, is relevant both in a post-emergency situation and within a risk-reduction policy. In the past an empirical model was proposed, involving the computation of a usability index based on macroseismic intensity and on seven building parameters, combined by means of regression coefficients and weights. The statistical model was calibrated on data of about 60 000 buildings affected by the 2009 L'Aquila earthquake in Italy. Therefore, it is useful to validate the model against data from the 2002 Molise earthquake in Italy. Good agreement between predicted and observed usability is shown, despite the fact that in 2002, macroseismic intensity was attributed to an entire municipality instead of a more limited area. Moreover, given the current availability of the shakemaps for the 2009 event, a novel model replacing conventional macroseismic intensity by an instrumental intensity measure is proposed. Three ground motion parameters are considered here: peak ground acceleration, peak ground velocity, and spectral pseudoacceleration at a period of vibration of 0.3 s. The model has been streamlined by reducing the building parameters from seven to five: building position within the structural aggregate, roof type, construction timespan, structural class, and pre-existing damage to structural elements. Peak ground acceleration and spectral pseudoacceleration are shown to be less effective than peak ground velocity in predicting observed usability. Therefore, usability probability matrices are computed in terms of peak ground velocity; the model is presented with all necessary coefficients and weights, and a worked-out example shows how to apply the procedure.

Keywords: seismic vulnerability, building parameters, usability probability matrices, PGA, PGV, spectral pseudoacceleration.

1 INTRODUCTION

In recent years, earthquakes have brought about a great number of casualties and economic loss. In particular, unreinforced masonry buildings, which represent a large percentage of the building stock, are usually greatly affected. Consequently, seismic risk reduction becomes fundamental for well-considered management of available economic resources. The different methodologies present in literature can be classified as empirical, mechanical or hybrid (Calvi et al. 2006), and they are all aimed at the generation of damage probability matrices (Whitman et al. 1973; ATC-13 1985) or fragility curves (Spence et al. 1992; Rota et al. 2008). An extended state of the art for unreinforced masonry buildings vulnerability methods has been presented by D'Ayala (2013), according to whom the empirical methods, developed over the last 35 years, can be regrouped into: i) categorisation of buildings into typological classes (Rota et al. 2011), with a specific propensity for damage and representative of the constructions present in the area, and ii) score methods, based on the computation of a vulnerability index, function of several buildings parameters (Benedetti and Petrini 1984; Lagomarsino and Giovinazzi 2006; Vicente et al. 2011; Ferlito et al. 2013). More recently, mechanical methods have become widespread, as a consequence of increased computational capacities that lead to the development of more complex and refined numerical models (Erberik 2008; Borzi et al. 2008; D'Ayala 2013; Mouyiannou et al. 2014). Even in this case, two principal methods, based on the performance-based design, can be taken into account to evaluate the seismic vulnerability assessment of existing buildings: i) association between capacity and demand curves in terms of spectral acceleration or displacement, e.g. N2 method (Fajfar 2000), ii) association between damage thresholds and damage index. Experimental tests are required to validate the analytical/mechanical methods and to calibrate the parameters set in the numerical analyses. Finally, hybrid methods combine analytical methods with post seismic observed data for the probabilistic definition of mechanical and structural characteristics and for the statistical treatment of the uncertainty in intensity measures and vulnerability parameters (Barbat et al. 1996; Kappos et al. 2006).

All previous works investigate damage in unreinforced masonry buildings. However, a relevant performance indicator is building usability (Stannard et al. 2014), intended as the quality of a building being habitable or occupiable (Gebelein et al. 2017) after a seismic event. In particular, the initial reconstruction process after the 2009 L'Aquila earthquake in Italy used usability classification as criterion for repair funding allocation, as discussed by Rossetto et al. (2014) and Di Ludovico et al. (2017a; 2017b). Rosti et al. (2018) analyzed the frequency of usability outcomes in the L'Aquila database for masonry, reinforced-concrete, steel, and mixed-structure buildings, and they correlated different damage indexes with the usability classifications, a point already mentioned by Rota et al. (2008). For the same earthquake, Bertelli et al. (2018) defined fragility curves in terms of usability rates for different building classes, given the peak ground acceleration (PGA) derived either from shakemaps or from ground motion prediction equations. Finally, with reference to the 2016-2017 Central Italy seismic sequence in the historical center of Norcia, Sisti et al. (2018) highlighted several correlations between structural and geometric characteristics and usability performance.

The intensity-measure selection represents a relevant issue in all models, with macroseismic intensity (Lagomarsino and Giovinazzi 2006; Zuccaro and Cacace 2015) and PGA (e.g. Del Gaudio et al. 2017; Rosti et al. 2018) being the most common choices. Whereas PGA is an instrumental measure, macroseismic intensity is a conventional estimation of ground shaking severity on the basis of observed effects in a limited area (Grünthal 1998).

In a previous work related to the L'Aquila data, Zucconi et al. (2017) proposed an empirical model for usability assessment. As summarized in Section 2, an index is calculated as a weighted sum of seven structural parameters, given the macroseismic intensity, according to rigorous statistical techniques. In order to test the robustness of the model for a different set of constructions, data surveyed after the 2002 Molise earthquake in Italy is considered in Section 3, obtaining

a rather promising agreement. Moreover, the Italian National Institute of Geophysics and Volcanology has recently published, for each seismic event starting from 2008, the raw data of shakemaps in terms of different ground motion intensity measures (http://shakemap.rm.ingv.it/shake/index.html). Thus, Section 4 presents novel usability assessment models calibrated on data from the 2009 L'Aquila earthquake, replacing the conventional macroseismic intensity with an instrumental intensity measure, either the PGA, or the peak ground velocity (PGV), or the spectral pseudoacceleration at a period of vibration equal to 0.3 s ($S_a \mid T = 0.3$ s). Comparison between predicted and observed usabilities makes it possible to select the most effective intensity measure and a worked-out example presents a step-by-step application of the proposed model.

2 SUMMARY OF THE USABILITY ASSESSMENT MODEL BASED ON MACROSEISMIC INTENSITY

As customary in Italy, at least since the 1997 Umbria-Marche earthquakes (Pinto and Taucer 2007), also after the 2009 L'Aquila earthquake, buildings were inspected by firefighters, university researchers and practitioners who assessed if their use was safe or not. Surveys were performed of approximately 75 000 buildings, 60 000 of which had an unreinforced masonry structure, and data were collected with the "Level 1 Form for Post-Earthquake Damage and Usability Assessment and Emergency Countermeasures in Ordinary Buildings" (Italian acronym AeDES) (Pinto and Taucer 2007).

Building inspection entailed the rapid visual survey of geometrical, structural and damage information (Baggio et al. 2007), leading to an assessment of six usability classes: A, usable building having no or only light damage; B, temporarily unusable building, but usable with short-term countermeasures; C, partially unusable building, wherein the heavy damage is limited to a portion of the construction and independent safe use is possible in the other parts of the building; D, temporarily unusable building requiring a more detailed inspection; E, unusable building due to extensive medium damage or severe damage even if limited to a small portion of the construction; F, unusable building for external risk, posed by close-by buildings and/or geotechnical concerns.

Based on the 2009 L'Aquila earthquake data, Zucconi et al. (2017; 2018a) developed a model to forecast the usability of unreinforced masonry buildings that is briefly described in this section. Because no other ground motion parameters were available at that time, the model resorted to the Mercalli-Cancani-Sieberg macroseismic intensity, I_{MCS}, customary in Italy (Musson et al. 2010).

For each macroseismic intensity degree, a usability index U was defined as follows:

$$U|I_{MCS} = \frac{\sum_{i=1}^{p}(u_i|I_{MCS})w_i}{\sum_{i=1}^{p} w_i} = \sum_{i=1}^{p}(u_i|I_{MCS})\overline{w}_i \quad [1]$$

where: $u_i|I_{MCS}$ is the loss-of-usability coefficient corresponding to the i-th of the p considered building parameters, w_i is the weight of the i-th parameter, and $\overline{w}_i$ is its corresponding normalized value. The loss-of-usability coefficient u_i varies between 0 and 1, with 0 being a completely usable building and 1 a fully unusable building. This coefficient was computed as:

$$u_i|I_{MCS} = \frac{N_{UB,i}|I_{MCS}}{N_{TB,i}|I_{MCS}} \quad [2]$$

where: N_{UB} is number of equivalent unusable buildings, N_{TB} is the total number of buildings, and they were evaluated for each category of each building parameter listed further below. First of all, in order to define the number of equivalent unusable buildings, the six usability categories of the AeDES form were reduced to just three: F buildings were considered

equivalent to A buildings, because the proposed model cannot account for external risk; C buildings were considered equivalent to B buildings because the same repair contribution was granted to these two categories (Dolce and Manfredi 2015); D buildings were considered equivalent to E buildings because in the Authors' experience, the more detailed inspection usually ended up with an E assessment. In any case D, buildings were less than 1% of the sample, thus only marginally influencing the following computations. The number of equivalent unusable buildings used to compute u_i was given by the number of E buildings plus 0.3 times the number of B buildings. This 0.3 factor was the result of average repair contribution of a B building being equal to 30% of repair contribution of an E building (Dolce and Manfredi 2015). A careful estimation was necessary also for the total number of buildings used in the computation of u_i, otherwise an overrepresentation of unusable buildings would have occurred, as observed in other large scale assessments (Walsh et al. 2017). In fact, systematic inspections were carried out only in the epicentral area, whereas in more distant areas buildings were inspected only at the owner's request. Owners tended to present such requests only if the building was damaged and they could apply for a repair contribution. Therefore, the total number of buildings could not be estimated just from AeDES forms but needed to be approximated based on census data according to a detailed procedure described in Zucconi et al. (2018a), which involved Monte Carlo simulations and delivered a database comprising a total of approximately 110 000 unreinforced buildings. Finally, loss-of-usability coefficient values were fitted according to single-variable regressions.

Weights w_i of Equation *[1]*, also called loadings within a statistic framework, were determined by means of a principal component analysis (PCA), a methodology already applied in earthquake engineering (Gutiérrez and Zaldivar 2000; Aschheim et al. 2002; Ni et al. 2006; Loh et al. 2016; Massumi and Gholami 2016). According to Jolliffe (2002), PCA aims to reduce the dimensionality of a database encompassing a large number of possibly interrelated variables, while upholding the variation in the data as far as possible. Linear PCA entails an orthogonal linear transformation into a new set of variables, the principal components, which are uncorrelated and which are sorted in descending order as for explained variance, i.e. the proportion to which the model accounts for the variation in the dataset. The weights are the eigenvector coefficients that are the solution of the eigenvalue problem associated with the linear transformation of variables.

The variables present in the dataset allowed defining the following seven building parameters:

1. building position within the structural aggregate;
2. number of stories above ground;
3. construction timespan;
4. structural class;
5. presence of strengthening interventions;
6. roof type;
7. pre-existing damage to structural elements.

Within a descriptive statistics framework, data related to the 2009 L'Aquila database were categorical, i.e. recording qualities or characteristics of the inspected buildings, such as the position within a block or the type of vertical structures. Even when numbers are involved, such as for the number of stories or the age of the construction, they do not have real numerical meaning and no direct mathematical operation is applicable. According to a statistical language, categories correspond to the choice options presented by the AeDES form for each building parameter. For each of the previous seven parameters, the relevant categories were identified, as explained below.

The parameter “building position within the structural aggregate” considered four categories that described the feature of a construction being either isolated or belonging to a block, in which case the internal, end-of-row and corner positions are possible. There have been reports of building position influencing earthquake performance (Giuffrè 1996; Ramos and Lourenço 2004), thus recommending its consideration in the model. The parameter “number of stories above ground”, obtained as the difference between the total number of stories and the number of basement stories present in the AeDES form, was described by three categories: 1 story, 2 stories, more than 2 stories. This parameter was used to define building types within empirical fragility models (Rota et al. 2008; Rota et al. 2011). The timespan within which the construction took place can be relevant because of both aging effects (Zuccaro and Cacace 2015) and building codes in force at the time of construction (Sorrentino 2007). Because of substantial changes in Italian standards, the following categories were considered: < 1919, 1919-1945, 1946-1961, > 1961 (Zucconi et al. 2018a). The idea of classifying buildings in terms of structural classes was already proposed by several authors (e.g., Braga et al. 1982; Dolce and Goretti 2015). Based on Zucconi et al. (2018a), four structural classes were defined as a combination of vertical and horizontal structures (Table 1). No explicit role was attributed to connections such as ring beams or tie rods. Although these details strongly influence the earthquake performance of unreinforced masonry buildings (Magenes et al. 2014; AlShawa et al. 2019), they were frequently covered by plaster and flooring, so that they may escape a rapid visual screening. A similar comment applied to strengthening interventions, which can be crucial for earthquake performance (Lagomarsino and Giovinazzi 2006; Abrams et al. 2017), but for which at most a generic presence (or an absence) can be identified from just a visual inspection, considering only two categories. The roof-type parameter was described by the four categories within the AeDES form: thrusting heavy, non-thrusting heavy, thrusting light and non-thrusting light. The first adjective concerned the statical scheme, which can either involve or not a thrust on the supporting walls, influencing the seismic response (Sorrentino et al. 2008). The second adjective was referred to the roof construction technique, which was usually timber (light) in historical buildings and reinforced concrete (heavy) in modern ones, but could be reinforced concrete also in historical buildings as a consequence of replacement (Sorrentino and Tocci 2008). Finally, the parameter related to pre-existing damage described the condition of the building before the seismic event, which was reported as important vis-à-vis seismic behavior (Dolce and Goretti 2015; Colonna et al. 2017). The categories of pre-existing damage followed the six levels (from 0 to 5) of the European macroseismic scale (Grünthal 1998) and were obtained by taking into account extension and severity, as suggested by Goretti and Di Pasquale (2004).

Vertical structures / Horizontal structures	Not identified or poor quality masonry of irregular layout (rubble stones, pebbles, …)	Good quality masonry of regular layout (blocks, bricks, dimensioned stone units, …)
Not identified, vaults or beams with flexible slab (timber beams with a single layer of timber boards, jack-arch slab, …)	Structural class 4	Structural class 2
Beams with rigid or semi-rigid slab (timber beams with double layer of timber boards, I-beams and hollow tile blocks, reinforced concrete floors, beams well connected to reinforced concrete slabs, …)	Structural class 3	Structural class 1

Table 1. Structural classes (after Zucconi et al. 2018a).

Based on single-variable regression estimation of loss-of-usability coefficients u_i and on PCA estimation of weights $\overline{w}_i$ Zucconi et al. (2017) defined Usability Probability Matrices (UPMs) for each macroseismic intensity, considering three possible usability outcomes, corresponding to a building tagged as A = usable, B = partially unusable, E = unusable. A worked-out example presented in Section 4.4 for the new model, calibrated for ground motion intensity measures, will help the reader understand how the method was applied in this and in the following section considering macroseismic intensity.

3 VERIFICATION OF THE USABILITY MODEL WITH DATA FROM THE 2002 MOLISE EARTHQUAKE

A limitation of empirical models is their calibration for a specific set of buildings and a specific earthquake event. Therefore, it is useful to validate the model presented in the previous section, defined following the 2009 L'Aquila earthquake, with data from a different seismic event. The Italian Civil Protection Department has recently made public data collected after severe seismic events of the last decades (Dolce et al. 2017). Among them, the 2002 Molise earthquake, with a magnitude M_W 5.7, caused serious damage to buildings and a significant number of casualties, in particular near San Giuliano di Puglia, where I_{MCS} = VIII-IX was estimated. About 22 000 buildings in 75 municipalities (Figure 1) were surveyed with the AeDES form (Goretti and Di Pasquale 2004) in the post-emergency phase.

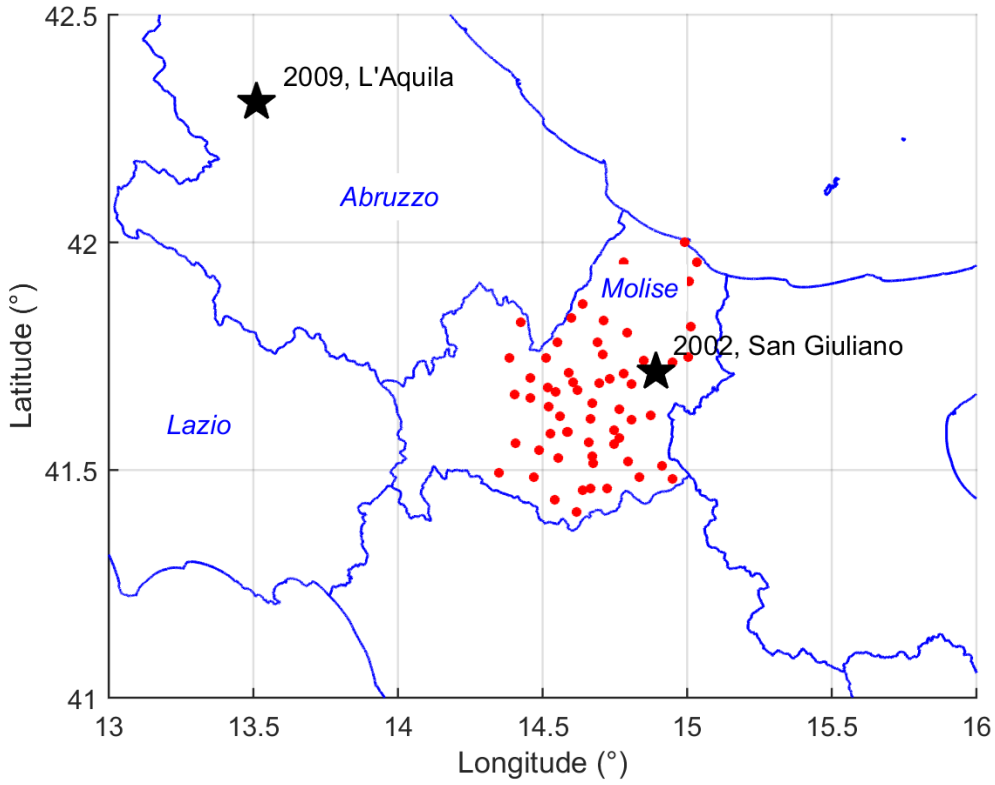

Figure 1 Location of the municipalities surveyed after the Molise earthquake.

The AEDES-form data were implemented in a Matlab (MathWorks 2016) environment and used to validate the usability model summarized in the previous section, selecting a subset of about 18 000 buildings, not taking into account forms:

- wherein buildings do not have a masonry structure;
- wherein the fields related to structural characteristics were not filled;
- wherein no usability outcome was reported;
- wherein damage level and usability outcome were contradictory (e.g., heavy damage associated with usability or no damage associated with an unusable building);
- related to a settlement where less than ten forms were filled, in order to avoid the overrepresentation of special buildings (town hall, museum, small factory and so on), while neglecting less than 0.2% of the original database;
- related to a municipality having I_{MCS} < V, because the model was calibrated assuming this lower bound.

The database of unreinforced masonry buildings inspected after the 2002 Molise earthquake comprises the disaggregation of construction timespan shown in Figure 2a. There is a prevalence of buildings older than one hundred years, while the most recent constructions, belonging to the category "> 1961", are less than 8%. The age breakdown of the Molise database is fairly similar to that of L'Aquila (Figure 2c). Figure 2b shows a similar disaggregation for structural classes. The least vulnerable category, structural class 1, accounts for about 22% of the sample, while the most vulnerable accounts for about 44%. The disaggregation in the L'Aquila database is again similar.

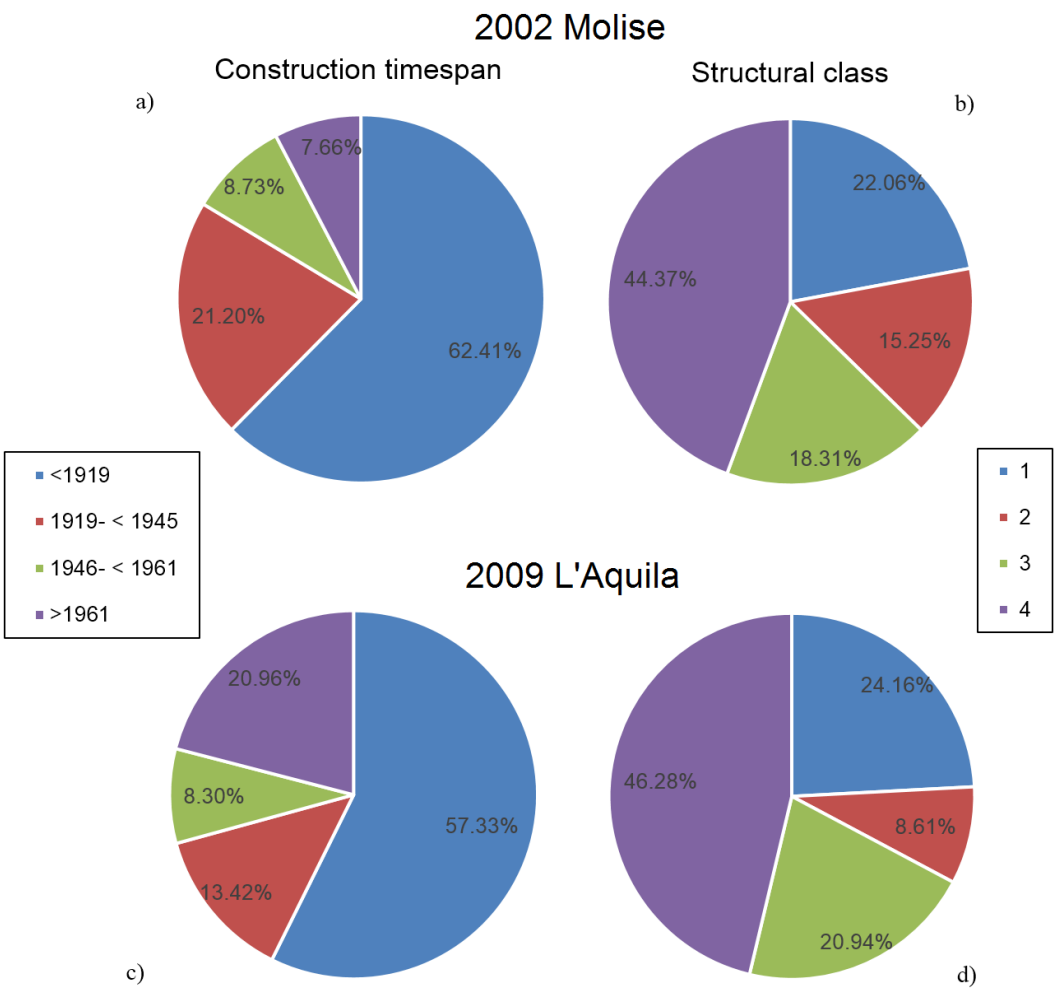

Figure 2 Database of unreinforced masonry buildings as a function of: construction timespan a) 2002 Molise c) 2009 L'Aquila; structural class b) 2002 Molise d) 2009 L'Aquila.

Despite these similarities, it is possible to recognize some differences in the construction features of the two databases. For instance, within structural class 1 buildings, rigid slabs account for 50% of the sample in Molise and 65% in L'Aquila (Figure 3a). Similarly, tie rods and tie beams are present in only 40% of the sample in Molise and 65% in L'Aquila (Figure 3b). Therefore, structural class 1 buildings in L'Aquila are, on average, slightly better built than in Molise. Considering structural class 4, vaults account for 37% of the sample in Molise and 52% in L'Aquila (Figure 4a). Similarly, tie rods and tie beams are present in only 5% of the sample in Molise and 19% in L'Aquila (Figure 4b). In this case, a more complex behavior can be expected depending on the type of vault present, with thin vaults being very vulnerable and robust vaults at ground floor displaying usually satisfactory performances (Sorrentino et al. 2018). Hence, despite both the Molise region and the province of L'Aquila belonging to the Apennine mountain range some differences in the building characteristics are present.

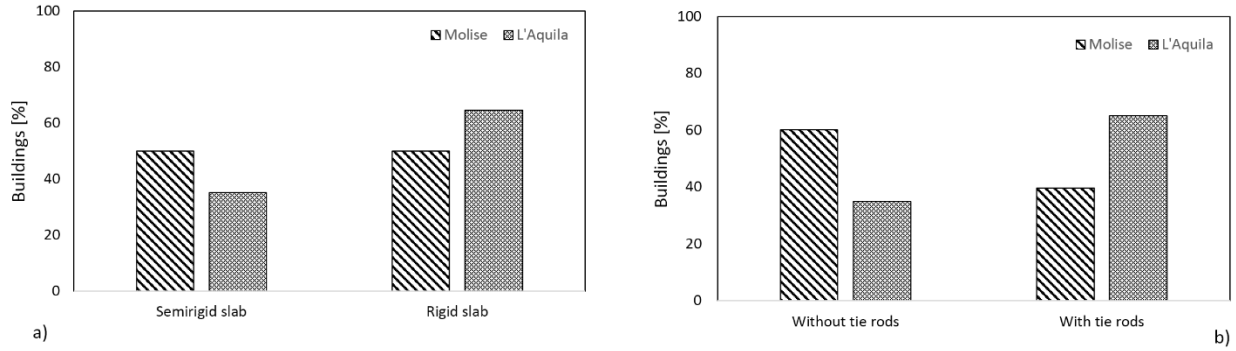

Figure 3 Comparison between the 2002 Molise and 2009 L'Aquila databases, in terms of: a) floor type, b) presence of tie rods. Structural class 1.

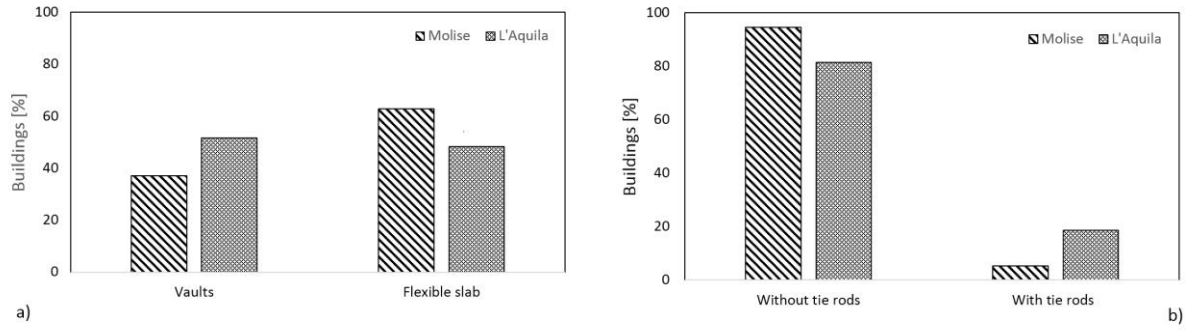

Figure 4 Comparison between the 2002 Molise and 2009 L'Aquila databases, in terms of: a) floor type, b) presence of tie rods. Structural class 4.

During the 2009 L'Aquila event, macroseismic intensity was given to individual settlements (Galli et al. 2009). Therefore, in the 90 surveyed municipalities 248 macroseismic intensities were attributed, with the city of L'Aquila alone having 56 districts and settlements. This procedure involved the definition of ground shaking severity related to a more limited area compared to what happened in 2002 in Molise, where a single macroseismic intensity was attributed to all settlements of a municipality (Locati et al. 2016).

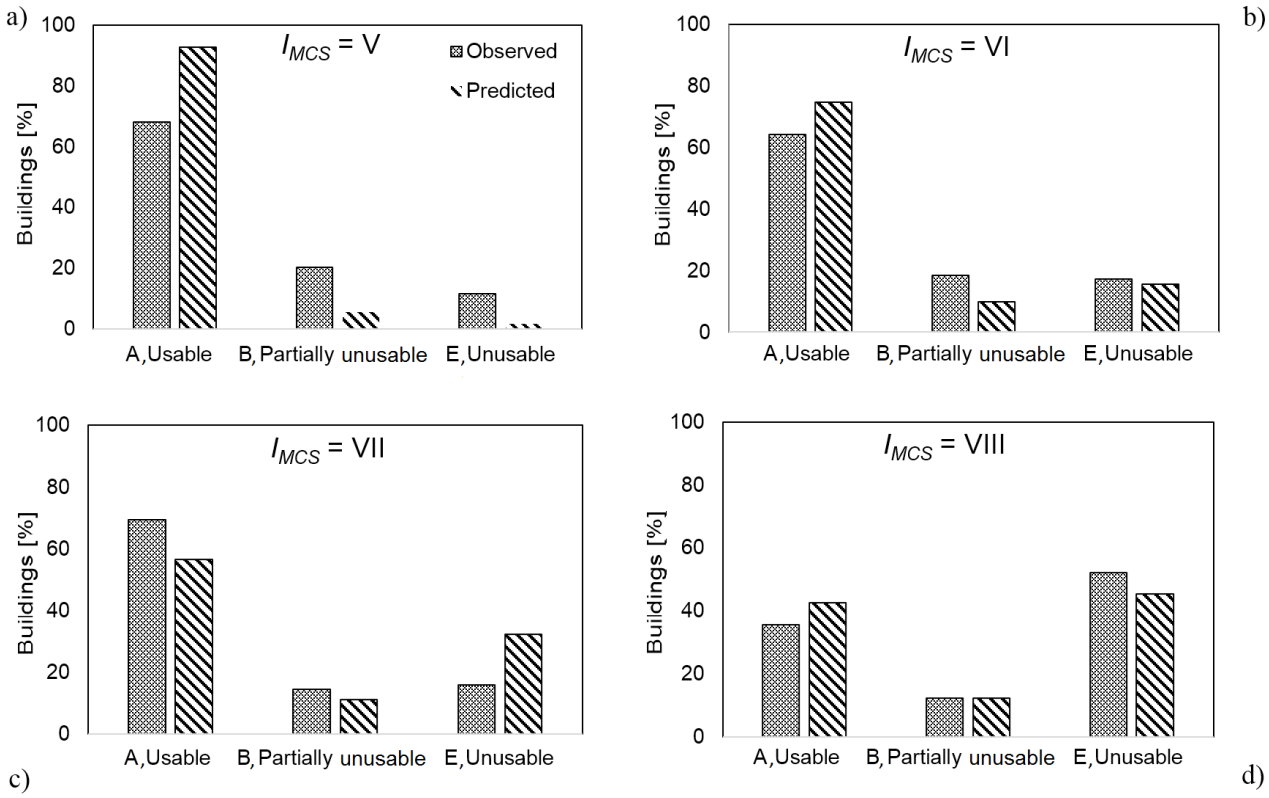

Figure 5 Comparison between observed and predicted usability outcome percentages, for different macroseismic intensities. Data related to the 2002 Molise earthquake

Based on the construction characteristics of each building and on the experienced macroseismic intensity, a usability outcome was predicted with the model presented in the previous section and compared with the one observed. Such a comparison, preliminarily presented by Zucconi et al. (2018b), is pursued systematically here and shown in Figure 5, disaggregating the building database in terms of usable, A, partially unusable, B, and unusable, E, as well as of macroseismic intensity I_{MCS}. Overall agreement is reasonable, especially for the highest intensity, where more unusable buildings occur. This agreement is systematic even if the dataset is further disaggregated, for instance in terms of structural classes (Figure 6).

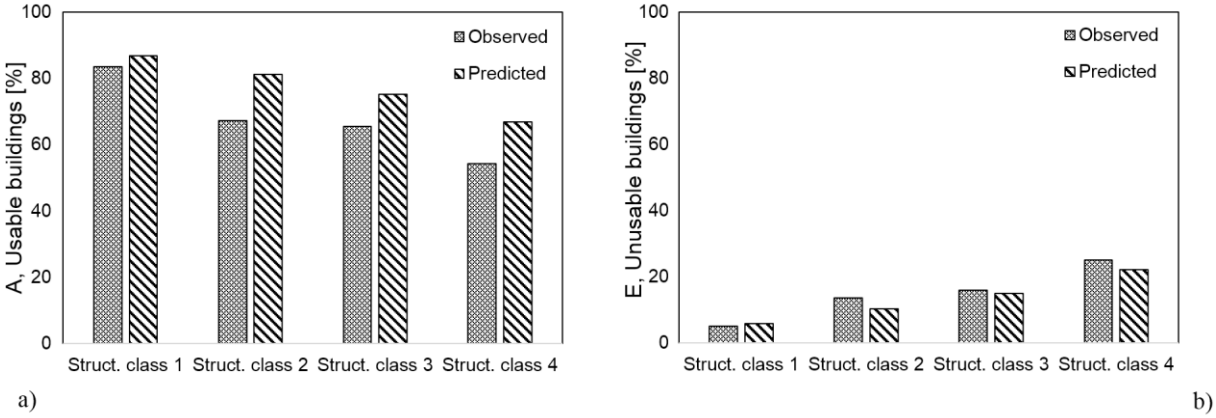

Figure 6 Comparison between observed and predicted percentages of: a) usable, and b) unusable buildings, for different structural classes. I_{MCS} = VI. Data related to the 2002 Molise earthquake.

Considering all intensities (Figure 7), predicted usable buildings account for 76% instead of 66%, partially unusable buildings make up 9% (18%) and unusable buildings are 15% (16%). Therefore, the model accurately predicts the relative frequency of unusable buildings, while for usable and partially unusable buildings leads to somewhat overconfident performances.

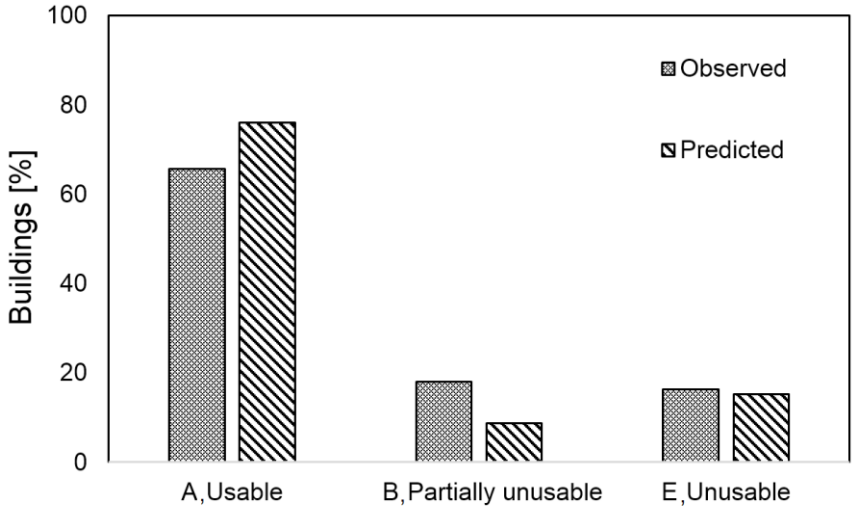

Figure 7 Comparison between observed and predicted usability outcome percentages considering all macroseismic intensities. Data related to the 2002 Molise earthquake.

The prediction error can be explained with both usability outcome and macroseismic intensity relying on expert judgment. Assigning a single macroseismic intensity to all the municipality settlements involves, at least for one of them, a significant deviation of actual ground motion severity in a limited area from the average ground motion severity. It is an inescapable fact that the usability outcome predicted by the model suffers from the poor definition of the macroseismic intensity experienced by each building. Finally, the differences in building characteristics shown in Figure 3 and Figure 4 inevitably affect the accuracy of a model calibrated for one area in predicting the performance of a different area.

4 CALIBRATION OF USABILITY MODELS CONSIDERING DIFFERENT GROUND MOTION INTENSITY MEASURES

The shortcomings of macroseismic intensity attribution, the use of different macroseismic scales adopted in world countries, and the lack of established hazard studies in terms of macroseismic intensity suggested using quantitative ground motion intensity measures. Although the instrument density of the Italian accelerometric network is far from guaranteeing at least one device for each settlement or district of larger centers, information about ground motion severity can be derived from shakemaps. Of course, it is important to emphasize that shakemaps can supply only approximate values because ground motion prediction equations and attenuation laws are used to fill the gaps between instruments, while often ground motion can vary markedly over short distances. In this way, the expected intensity measure depends on several factors that can introduce errors in the estimated values, in turn, influenced by inter-event variability (Dolce and Di Bucci 2014). Nonetheless, such approximations can still be considered acceptable in light of the limitations of macroseismic intensity.

The Italian National Institute of Geophysics and Volcanology has published the raw data (http://shakemap.rm.ingv.it/shake/1895389/products.html) related to the shakemaps of the 2009 L'Aquila earthquake (Faenza et al. 2011). Raw data is associated with the following ground motion parameters: i) PGA; ii) PGV; iii) $S_a \mid T$ = 0.3 s; iv) $S_a \mid T$ = 1.0 s; v) $S_a \mid T$ = 3.0 s.

Only the first three intensity measures are considered in the following. PGA is the most common intensity measure within empirical models and fragility functions (e.g. Del Gaudio et al. 2017; Rosti et al. 2018). PGV has been reported as being better associated with the seismic response of masonry buildings compared to acceleration measures (Mouyiannou et al. 2014). Finally, only the smallest period of vibration of the three considered within the shakemaps is meaningful. In fact, the buildings in this study with a number of stories above ground equal to one comprise 14% of the inventory, with two stories 46%, with three stories 33%, while less than 8% have more than three stories (Zucconi et al. 2018a). If the period of vibration is estimated according to the empirical formula in EC8-1 (EC8-1 2004), $T = 0.05\ H^{0.75}$ where H is the total building height in m, and an inter-story height equal to 3 m is assumed, T is approximately equal to 0.19 s for a two-stories building, and 0.26 s for a three-stories building. Therefore, the T = 0.3 s value is the closest one among the three available in the shakemaps.

PGA [g]		PGV [cm/s]		$S_a \mid T$ = 0.3 s [g]	
Bin	Category	Bin	Category	Bin	Category
< 0.05	0.025	≤ 5	2.5	< 0.10	0.05
0.05 - < 0.15	0.10	5 - < 15	10	0.10 - < 0.30	0.20
0.15 - < 0.25	0.20	15 - < 25	20	0.30 - < 0.50	0.40
0.25 -< 0.35	0.30	25 - < 35	30	0.50 - < 0.70	0.60
≥ 0.35	0.40	≥ 35	45	≥ 0.70	0.80

Table 2. Ground motion intensity measure bins and corresponding categories.

The shakemap PGA values vary in the range 0.02-0.48 g, with a step of 0.04 g; PGV varies between 2 to 58 cm/s (with a step of 2 cm/s), while the $S_a \mid T$ = 0.3 s varies in the range 0.04-0.88 g (with a step of 0.04 g). Intensity measure values have been aggregated into bins, with a 0.10 g step for PGA, a 10 cm/s step for PGV, and a 0.20 g step for $S_a \mid T$ = 0.3 s. Limited exceptions have been considered for the tail bins in order to meet practical limitations and avoid bins with very few data. The central value of each bin has been usually assumed as the categorical value of the bin, but the last categorical value is chosen to be close to the mean of available data. Slightly different values have been tested without getting any significant improvement in the results. Ground motion categories are summarized in Table 2.

Finally, it is worth emphasizing that the 2002 Molise earthquake shakemaps have not been released so far.

4.1 SINGLE-VARIABLE LOSS-OF-USABILITY REGRESSIONS

Depending on its location on the map, each building in the 2009 L'Aquila earthquake database was given a categorical value from Table 2 for each of the three ground motion intensity measures presented in the previous sub-section. Then, loss-of-usability regressions were derived for every one of the seven building parameters introduced in Section 2: building position within the structural aggregate, number of stories above ground, construction timespan, structural class, presence of strengthening interventions, roof type, pre-existing damage to structural elements.

After considering non-linear regressions, omitted here for the sake of brevity, linear expressions are assumed in order to avoid non-monotonic trends and limit intersecting curves. Unweighted regressions have been performed because the available database is considered representative of the actual building population (de Leeuw et al. 2012).

Since it is a survey form that is filled after a detailed inspection of the building, the AeDES form presents several categories for each parameter. In order to propose a simplified form to be used in preventive actions, Zucconi et al. (2018a) reduced the number of possible categories of building parameters. For instance, in the AeDES form there are thirty structural types but some of them occur in a very limited number of buildings or have performances very similar to other types. Therefore, Zucconi et al. (2018a) reduced them to just four structural classes. The categories of the parameters identified for macroseismic intensity and mentioned in Section 2 have been compared with possible alternatives but in the end they are the most effective also for the ground motion intensity measures considered here.

An example of loss-of-usability regression is shown in Figure 8 for building position within the structural aggregate and the three selected ground motion intensity measures. It is possible to observe that the least vulnerable condition is that of isolated building, whereas buildings belonging to a block show higher loss-of-usability coefficients. The most vulnerable positions are end-of-row and internal. This result is counterintuitive if compared with numerical model results (Ramos and Lourenço 2004; Formisano et al. 2011), but this trend can be explained by considering the association with other parameters. For instance, isolated buildings are newer than aggregated buildings and they belong to the less vulnerable structural class, while corner and internal buildings are older than end-of-row buildings and fall in the most vulnerable structural class. Regressions are similar for all intensity measures, and because this behavior is systematic, the following parameters are discussed in plots with PGV on the horizontal axis (Figure 9).

The number of stories above ground (Figure 9a) is relevant only when moving from single-story to multi-story constructions. Single-story buildings, which, as already mentioned, account for about 14% only of the sample, show a higher relative frequency of structural class 1, compared to two-story and more than two-story buildings, which have an almost coincident disaggregation in terms of structural classes, and account for about 86% of the portfolio.

The construction timespan shows clearly defined trends, with oldest buildings showing the worst performance (Figure 9 b). This behavior has been already observed (Zuccaro and Cacace 2015), and is related to a change in both geometry requirements and structural details. As for the first aspect, in 1962 the building code limited the spacing between transverse walls and the number of stories (L 1962). As for construction practice, the older the building the easier it is to find occurrences of poor masonry and flexible floors, with a large proportion of the portfolio falling in structural class 4, the most vulnerable.

The structural class, combination of vertical and horizontal structures (Table 1), greatly influences the loss-of-usability coefficients u_i (Figure 9c). Structural class 1 buildings have at most a loss-of-usability coefficients of about 20% even for PGV of about 45 cm/s. On the contrary, structural class 4 can reach 70%. Observed trends are fully intuitive, with good quality masonry and stiff floors contributing to a more satisfactory performance. The definition of structural classes in Table 1 is consistent with the model assuming macroseismic intensity as intensity measure, as presented in Section 2. However, analyses not shown here for the sake of conciseness highlighted that definitions other than those in Table 1 are less satisfactory. It is certainly counterintuitive that the proposed model does not account for the presence (or lack) of tie rods and ring beams but, as already mentioned, these details are not always visible to the naked eye, so that it is better to remove them at all from the empirical model.

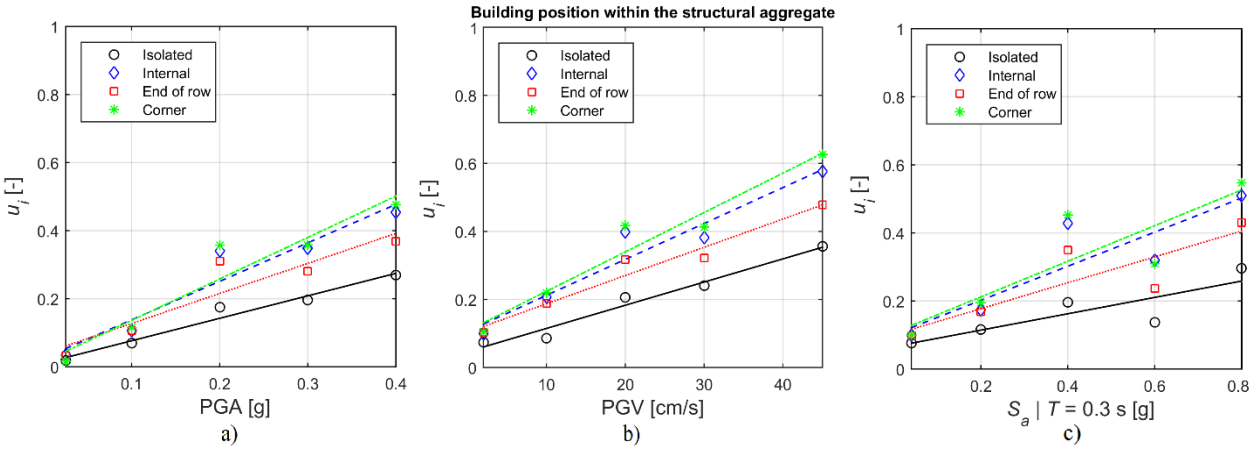

Figure 8 Building position within the structural aggregate loss-of-usability regressions for different ground motion intensity measures. Data related to the 2009 L'Aquila earthquake.

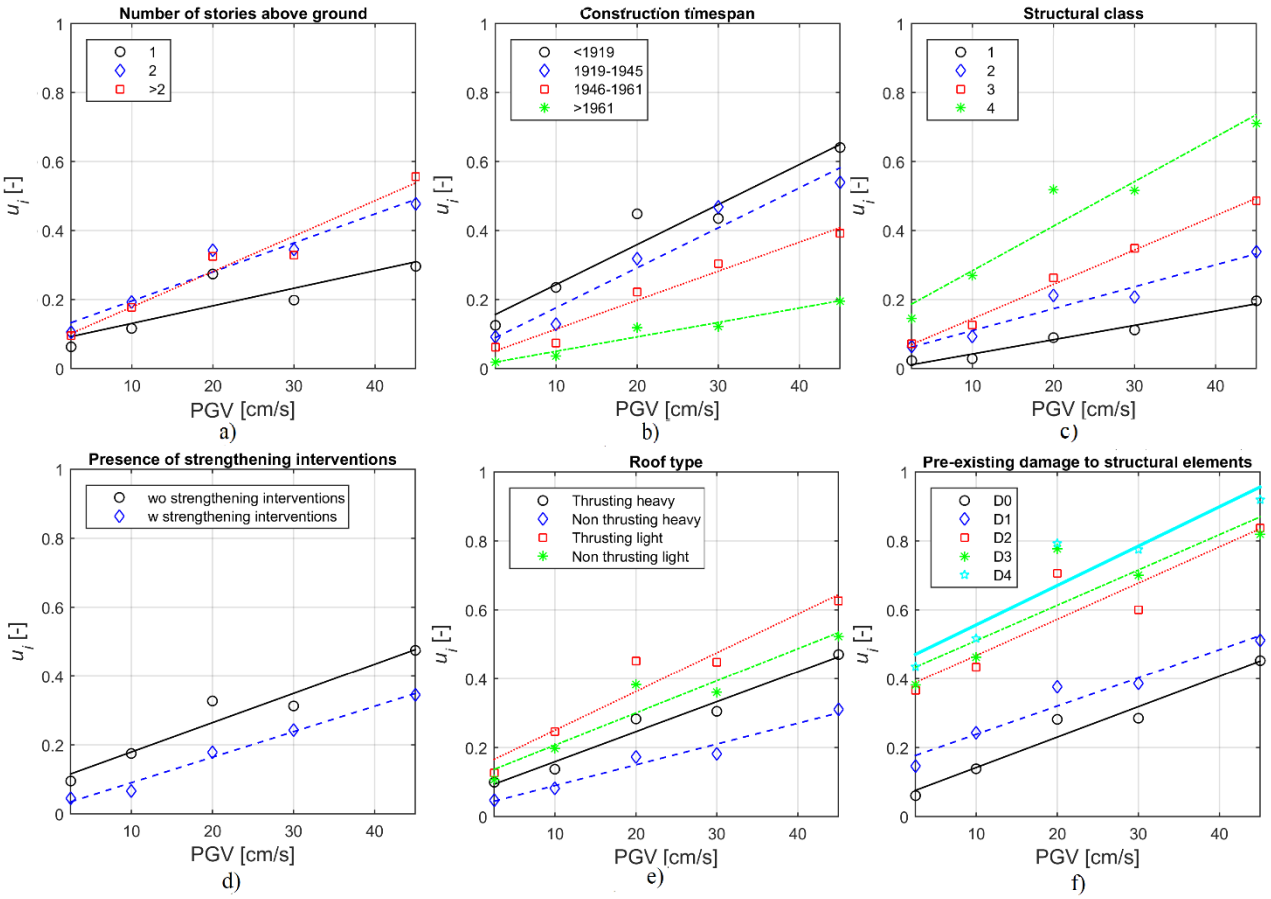

Figure 9 Loss-of-usability regressions for PGV: a) number of stories above ground, b) construction timespan, c) structural class (Table 1), d) presence of strengthening interventions, 6) roof type, f) pre-existing damage to structural elements. Data related to the 2009 L'Aquila earthquake.

Strengthening interventions are grouped into the following categories in the AeDES form: 1) injections or unreinforced coating; 2) reinforced masonry or masonry with reinforced coating; 3) other or unidentified strengthening. As for tie beams, it is usually rather difficult to recognize the presence or lack-of such interventions during a rapid visual inspection. Hence, just two categories are shown in Figure 9d. Moreover, the difference in the usability rate due to strengthening is somewhat more limited than one can anticipate. Again, the fact that several interventions are expected to escape being noticed in usability surveys makes it difficult to properly account for this parameter.

The roof type has a distinct impact on usability performance (Figure 9e), and the best condition is that of a non-thrusting and heavy roof. Although it is to be expected that a non-thrusting statical scheme is preferred, one might have expected a light top structure to be preferable. However, the adjective heavy refers to recent reinforced-concrete roofs, somewhat easier to connect to the top of masonry walls. This behavior was highlighted by the detailed analysis of the seismic performance of Norcia in 2016 (Sisti et al. 2018), provided that the walls are strengthened at the same time of roof replacement. Otherwise, catastrophic collapses may occur, especially if the intermediate floors are inserted in the existing walls, reducing their effective thickness (Augenti and Parisi 2010). Moreover, reinforced-concrete diaphragms are more frequent in newer buildings and are, thus, associated with better performances. On the other hand, a light roof structure can be rather old, hence, producing almost no diaphragm effect and having joists simply inserted in wall pockets.

As for pre-existing damage, regressions are clustered in two bundles (Figure 9f): no or light damage (D0, D1), or moderate to very heavy damage (D2, D3, and D4). No information is available for D5 pre-existing damage level, as one can expect, this being the condition of a collapsed building. Pre-existing damage is fairly relevant to explain damage observed for low levels of shaking, for which, all other things being equal, one would expect a low level of damage if the construction was not already damaged. The role of pre-existing damage in explaining unexpected and outlying post-event damage levels has been highlighted by Rosti et al. (2018) and is worth being part of the usability model.

Loss-of-usability coefficient regression values are reported in Appendix A for PGV as intensity measure and their use will be presented with reference to a worked-out example.

4.2 WEIGHTS EVALUATIONS BY MEANS OF PRINCIPAL COMPONENT ANALYSIS

Once the loss-of-usability coefficients u_i were computed, a PCA was performed in order to evaluate the weights $\bar{w}_i$ necessary to implement Eq. [1]. Fifteen PCAs were carried out, one for each of the five categories of the three ground motion intensity measures in Table 2. Each analysis was implemented taking into account the seven building parameters discussed in the previous sub-section. Every PCA delivered seven principal components, with the first being the most relevant, with an average explained variance of about 50% for all ground motion intensity measures (Figure 10). Consequently, hereinafter, the weights definition is based only on the first component.

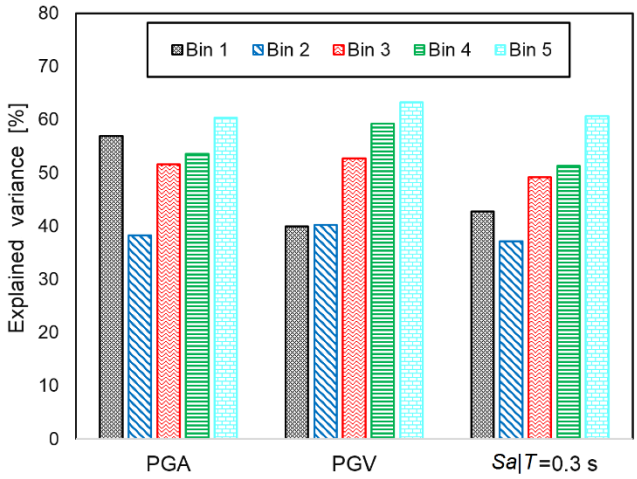

Figure 10 Variance explained by the first principal component delivered by the PCA, for each category associated with ground motion intensity measures' bins in Table 2. Data related to the 2009 L'Aquila earthquake.

The estimated weights $\overline{w}_i$ are almost constant for large values of the intensity measures, whereas for lighter shaking they are influenced by pre-existing damage (Figure 11). This parameter shows a marked decreasing trend with increasing intensities, consistently with the great relevance that high levels of previous damage have on overall damage surveyed in light shaking areas, as highlighted already by Rosti et al. (2018). Conversely, the weights associated with the parameters of number of stories above ground and presence of strengthening systematically give readings close to zero (Figure 11), highlighting the little importance they have for the usability model. This trend was observed already in the macroseismic intensity model, where such weights are equal on average to 0.041 and 0.020 (Zucconi et al. 2017). In the case of the number of stories, this outcome can be related to the association with more relevant parameters. Figure 12 shows that the disaggregation of the number of stories' categories (1, 2, > 2) in terms of construction timespan and structural class is very similar for a number of stories greater than 1. This observation is consistent with the loss-of-usability coefficients presented in Figure 9a, again very similar for buildings having 2 or more than 2 stories above ground. Additionally, these two categories account for more than 85% of the database, thus reducing the relevance of single-story buildings on the overall performance of the model. As for the presence of strengthening interventions, since identification may escape a visual inspection, the impact on usability is not systematic.

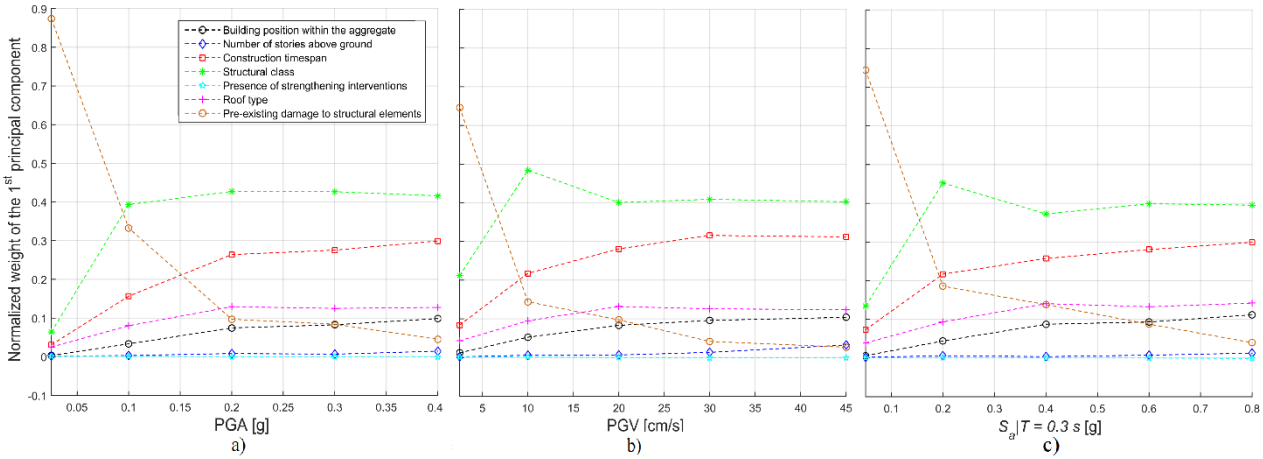

Figure 11 Normalized weight, $\overline{w}_i$, varying ground motion intensity measures and seven building parameters. Data related to the 2009 L'Aquila earthquake.

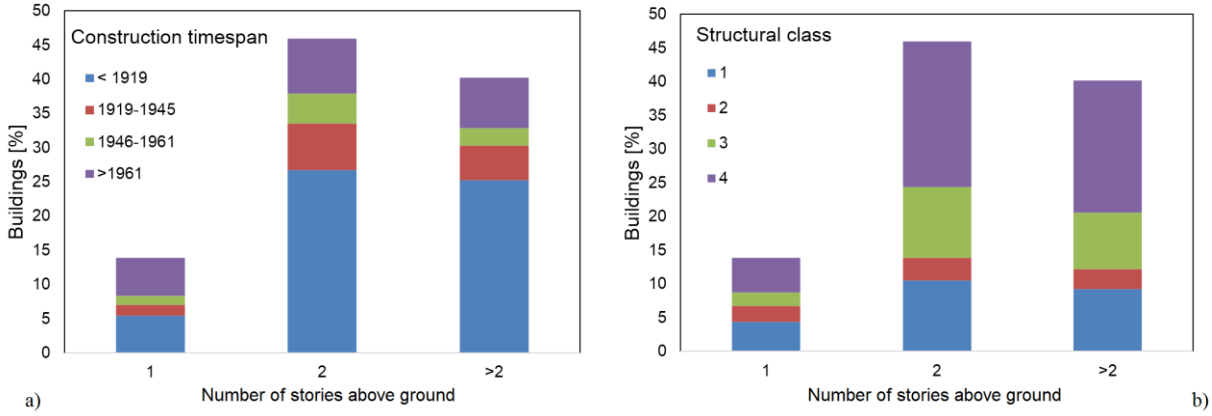

Figure 12 Disaggregation of number of stories' categories (1, 2, >2) in terms of: a) construction timespan and, b) structural class. Percentage computed over the total number of buildings in the dataset. Data related to the 2009 L'Aquila earthquake.

In view of these considerations, the usability models have been simplified, excluding the number of stories above ground and the presence of strengthening interventions, without sacrificing the explained variance. Thus, the PCAs have been repeated and the weights of the remaining five parameters have been updated, with minimal variations compared to Figure 11. The normalized weight, $\overline{w}_i$, to be used in Eq. [1] has been computed as mean value for all categories associated with the bins of each ground motion intensity measure in Table 2, thus delivering a constant value for each parameter independently from the ground motion level. The computation of a single value simplifies the model and avoids extrapolation for ground motions intensities greater than observed. Additional simulations mentioned in the following sub-section suggest that taking into account weights varying with shaking intensity only marginally improves the model while complicating it substantially. Normalized weights, $\overline{w}_i$, are shown in Table 3 and it is possible to notice that, for all intensity measures, the most important parameter is the structural class and the least important, but still not negligible, are building position within the structural aggregate and roof type. Construction timespan and pre-existing damage to structural elements, although figures are not too different, can be the second-most or third-most important parameter, depending on the selected intensity measure. Of course, this outcome is related to the same building falling into different categories, changing the intensity measure. Therefore, an overall assessment of the most effective model needs to consider weights and ground motion intensity measure at the same time, as will be done in the following sub-section.

Parameter	Building position within the structural aggregate	Construction timespan	Structural class	Roof type	Pre-existing damage to structural elements
PGA	0.059	0.207	0.348	0.098	0.288
PGV	0.071	0.245	0.387	0.106	0.192
$S_a \mid T = 0.3$ s	0.069	0.227	0.353	0.110	0.240

Table 3 Normalized weight, $\overline{w}_i$ (Eq. [1]), according to different ground motion intensity measures and building parameters.

4.3 USABILITY PROBABILITY MATRICES

Having defined the loss-of-usability coefficients u_i and the normalized weights $\overline{w}_i$, it was possible to evaluate the usability index for the considered ground motion intensity measures: $U|\text{PGA}$, $U|\text{PGV}$, and $U|S_a|T = 0.3\ s$, by means of Eq. [1]. For each category of ground motion intensity measures, the usability index U was computed by taking into account, for every building parameter, the smallest and largest figures of the loss-of-usability coefficients defined in Section 4.1. Thus, a lower and an upper bound were determined for U and this range was divided into five equispaced bins, whose readings are presented below. For each intensity measure category and each U bin, the relative frequencies of observed E (unusable) buildings were computed and fitted with linear regressions to smooth distributions (Figure 13a). Then, observed A (usable) relative frequencies underwent a multivariate fitting, given ground motion intensity and E regression values (Figure 13b). Finally, B relative frequencies are set so that A + B + E = 100% (Figure 13c).

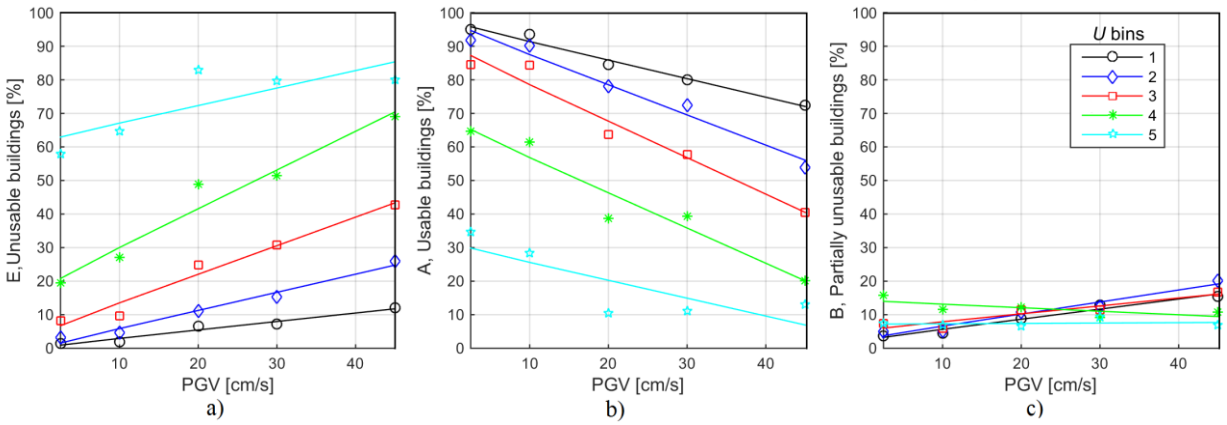

Figure 13 Regressions of relative frequency distributions of observed buildings: a) unusable buildings (E); b) usable buildings (A). c) Regressions and relative frequency distributions of observed partially unusable buildings (B). Data related to the 2009 L'Aquila earthquake.

Fitted values represent usability probability matrices, an example of which is given in Table 4 in terms of PGV. Within a given category of PGV, the five *U* bins can be interpreted as categories characterized by an increasing loss of usability. Additionally, as a consequence of performed regressions, moving from a PGV category to a larger one involves a linear increase of the probability of a building being unusable. This trend helps explaining why usability index *U* ranges from 0 toward 1 only across several intensity measure categories. As with the single-variable u_i coefficient, the *U* index expresses a loss of usability, thus it cannot be expected to have the same value for different ground motion shaking intensities.

PGV = 5 cm/s	A	B	E	PGV = 10 cm/s	A	B	E	PGV = 20 cm/s	A	B	E
U	[%]	[%]	[%]	*U*	[%]	[%]	[%]	*U*	[%]	[%]	[%]
0.030- < 0.070	95.8	3.3	0.9	0.070- < 0.122	91.4	5.6	3.0	0.120- < 0.184	85.8	8.7	5.5
0.070- < 0.110	94.5	3.8	1.7	0.122- < 0.174	87.4	6.6	6.0	0.184- < 0.248	78.4	10.2	11.4
0.110- < 0.150	86.7	6.0	7.3	0.174- < 0.226	78.1	7.9	14.0	0.248- < 0.312	67.3	10.3	22.4
0.150- < 0.190	64.0	14.4	21.6	0.226- < 0.278	55.9	13.5	30.6	0.312- < 0.376	45.7	12.3	42.0
0.190- < 0.230	29.7	7.1	63.2	0.278- < 0.330	25.4	7.3	67.3	0.376- < 0.440	20.1	7.4	72.5
PGV = 30 cm/s	A	B	E	PGV = 45 cm/s	A	B	E				
U	[%]	[%]	[%]	*U*	[%]	[%]	[%]				
0.180- < 0.256	80.3	11.7	8.0	0.260- < 0.356	72.0	16.2	11.8				
0.256- < 0.332	69.5	13.8	16.7	0.356- < 0.452	56.0	19.2	24.8				
0.332- < 0.408	56.6	12.6	30.8	0.452- < 0.548	40.5	16.2	43.3				
0.408- < 0.484	35.5	11.2	53.3	0.548- < 0.644	20.2	9.4	70.4				
0.484- < 0.560	14.9	7.5	77.6	0.644- < 0.740	7.0	7.7	85.3				

Table 4 Conditional probability of usability outcomes A (usable), B (partially unusable), E (unusable), varying PGV categories (Table 2) and usability index *U* (Eq. [1]) bins.

As with the comparison already introduced for the 2002 Molise earthquake data, from Figure 14 to Figure 16 observed usability outcomes are paralleled with outcomes predicted by means of the usability matrices. Matches are almost perfect if all categories are considered (subplot (f) in the three figures) and results are encouraging even for the third category of each intensity measure, where the difference between observation and prediction is always less than 7% for PGA, approximately 4% for PGV, and less than 9% for $S_a \mid T = 0.3$ s.

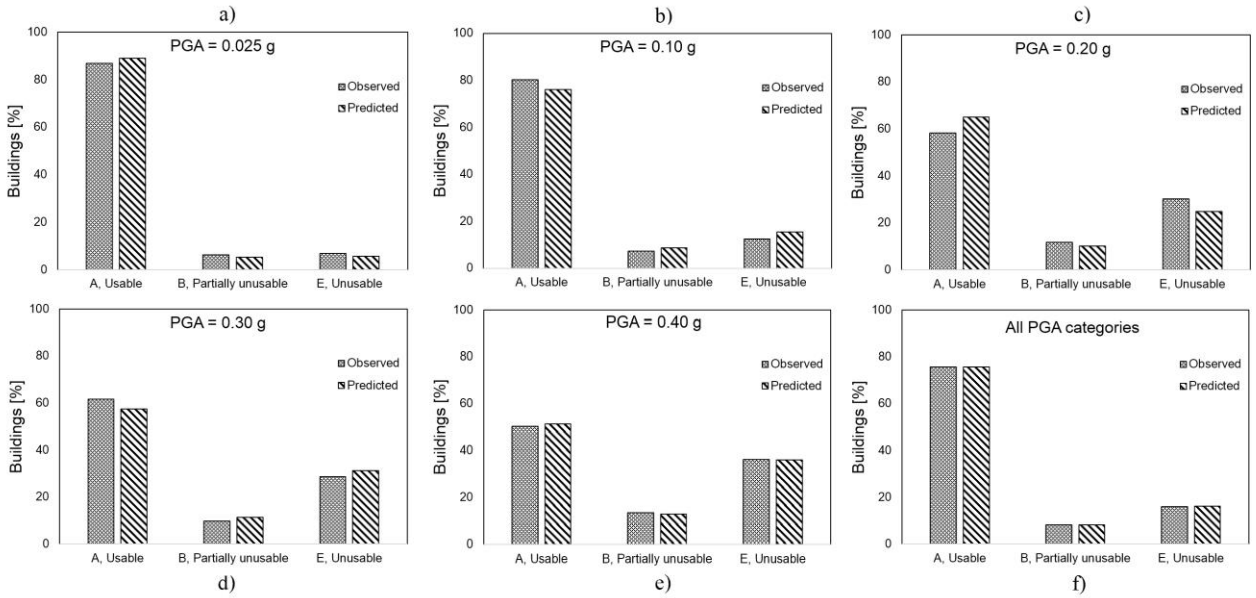

Figure 14 Comparison between observed and predicted usability outcome percentages, for different PGA categories (Table 2). Data related to the 2009 L'Aquila earthquake.

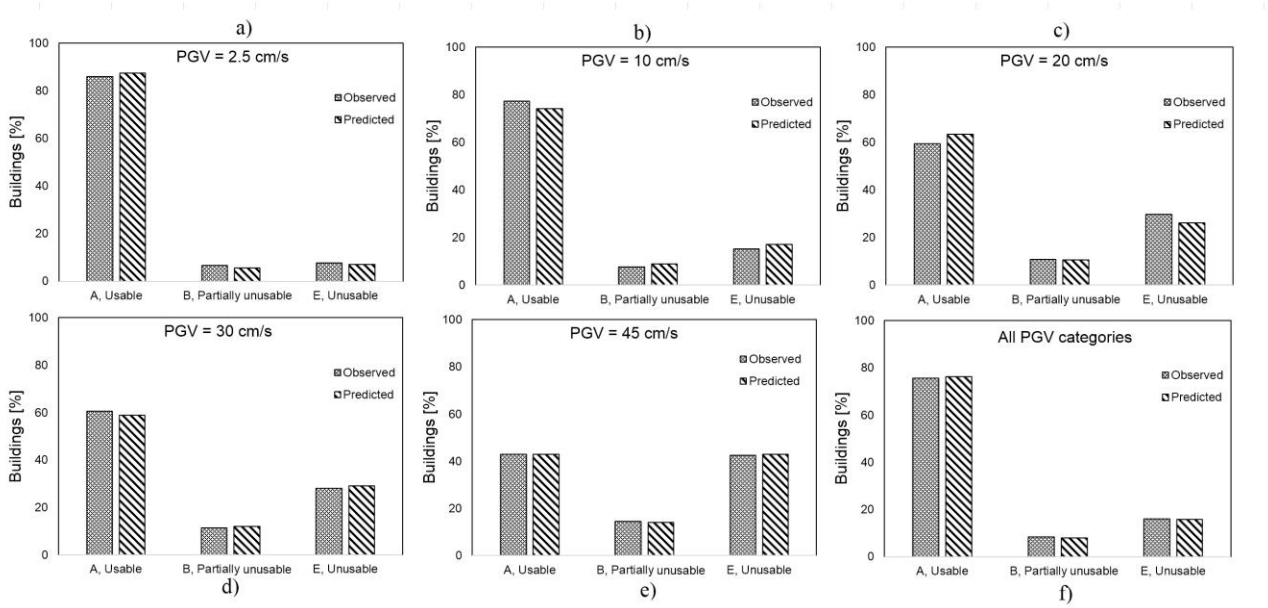

Figure 15 Comparison between observed and predicted usability outcome percentages, for different PGV categories (Table 2). Data related to the 2009 L'Aquila earthquake.

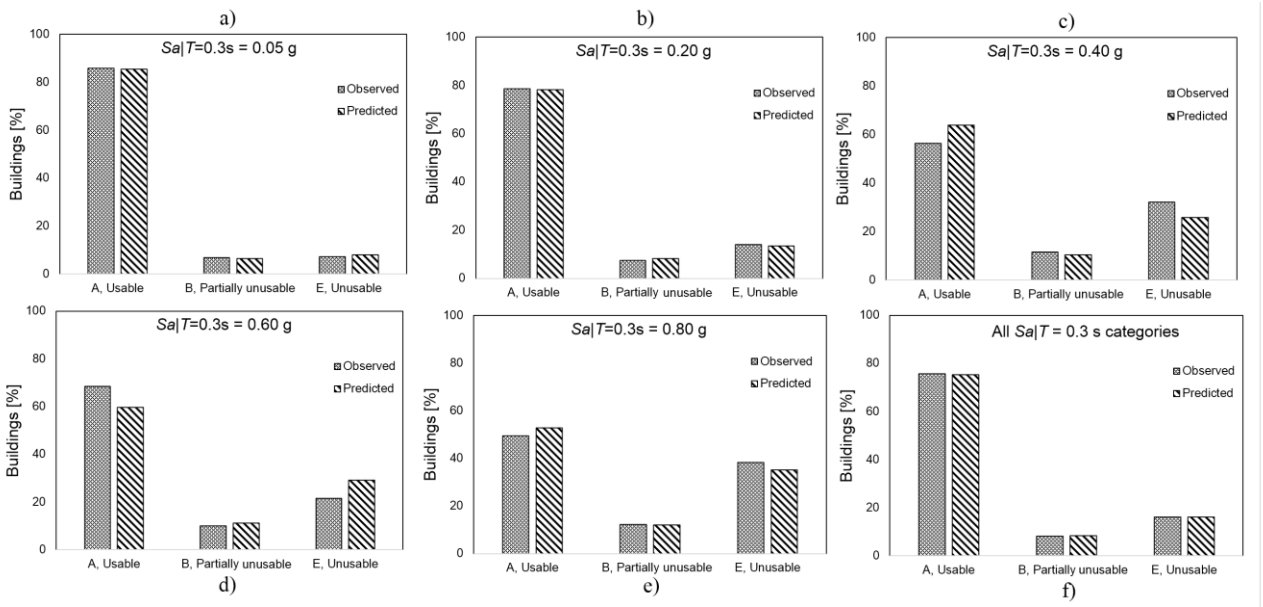

Figure 16 Comparison between observed and predicted usability outcome percentages, for different $S_a \mid T = 0.3$ s categories (Table 2). Data related to the 2009 L'Aquila earthquake.

In order to investigate further which intensity measure produces the best performance, the comparison is disaggregated by taking into account, within a single intensity category, the five U bins present in the usability matrices. Observed usability, $U_{observed}$, and model-predicted usability, U_{model}, are computed as average value for the buildings falling within a category of the ground motion intensity measure in Table 2 and within a bin of U in the usability matrices. The comparison between observation and prediction is shown in Figure 17, where data are clustered near the bisector line, emphasizing the reasonable agreement between $U_{observed}$ and U_{model}. Nonetheless, the points of same intensity measure category are aligned along curves with a steeper slope compared to the bisector, highlighting that the model sacrifices some of the data variance as a result of the simplifications introduced. The coefficients of determination with respect to the bisector line are fairly high, being equal to 0.65, 0.82 and 0.71, respectively, for the models based on PGA, PGV, and $S_a \mid T = 0.3$ s, hence PGV produces the best result in terms of coefficient of determination with respect to the bisector. Consequently, PGA and $S_a \mid T = 0.3$ s will be dropped hereinafter.

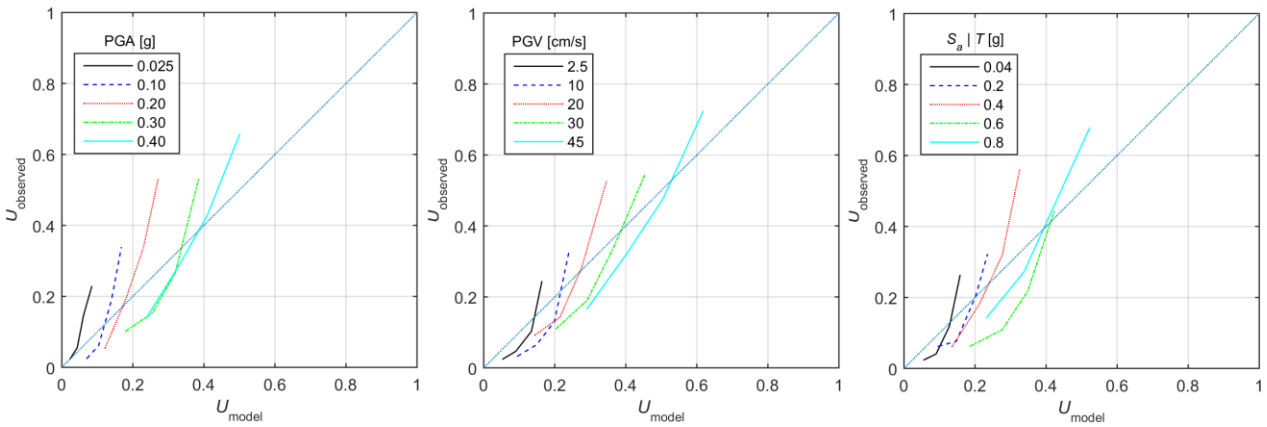

Figure 17 Comparison of average model usability index (Eq. [1]) with average observed usability, considering different ground motion intensity measures. Data related to the 2009 L'Aquila earthquake.

Several alternative intensity measures, *IM*, have been considered as linear combinations of previous ground motion parameters:

[3] $$IM = a\ \mathrm{PGA}' + b\ \mathrm{PGV}' + c\ S_a'|T = 0.3\ \mathrm{s}$$

where $'$ indicates normalization with respect to maximum recorded value, and $a, b,\ c$ are scalar coefficients investigated parametrically. No substantial gain in the agreement between model and observation has been obtained.

Additionally, instead of the mean values of Table 3, weights varying with the category of the intensity measure, $\overline{w}_i|I_i$, have been considered:

[4] $$U|I_i = \frac{\sum_{i=1}^{p}(u_i|I_i)(w_i|I_i)}{\sum_{i=1}^{p}(w_i|I_i)} = \sum_{i=1}^{p}(u_i|I_i)(\overline{w}_i|I_i)$$

where $I_i = \mathrm{PGA}, \mathrm{PGV}, \text{or } S_a|T\ =\ 0.3$ s, but again without any appreciable increase in the coefficient of determination. This result, somewhat surprising in light of the trends in Figure 11, can be explained considering that the usability index is defined not only by the weights but also by the loss-of-usability coefficients, which, given the intensity measure, vary from parameter to parameter. Additionally, for the first intensity measure category, where the pre-existing damage would be the most relevant parameter (Figure 11), very few buildings fall within the D3 and D4 categories and, hence, only negligibly affect overall results. This aspect should become clearer in the worked-out example presented in the next sub-section.

4.4 WORKED-OUT EXAMPLE

Usability probability matrices represent an important tool for scenario analyses and to simulate preventive measures because they allow us to estimate the number of homeless people and to simulate the effect of preventive measures, involving a change of structural class or of roof type or the removal of a pre-existing damage. In order to explain how the proposed model is applied, a worked-out example is discussed in this section.

A site having an expected PGV = 26 cm/s is considered, involving the use of the fourth PGV category = 30 cm/s in the tables of Appendix A. The assumed building:

1. is part of a structural aggregate and located in an internal position. Building position within the structural aggregate: internal, *u* = 0.423;
2. dates back to the 19th century. Construction timespan: < 1919, *u* = 0.476;
3. has irregular masonry and timber floors. Structural class: 4, *u* = 0.542;
4. has a reinforced-concrete pitched roof, with walls supporting both the ridge line and the eave lines. Roof type: non-thrusting heavy, *u* = 0.210;
5. has only light pre-existing damage. Pre-existing damage to structural elements: D1, *u* = 0.403.

Based on the weights in Table 3, the usability index is equal to:

[5] $$U = 0.423 \cdot 0.071 + 0.476 \cdot 0.245 + 0.542 \cdot 0.387 + 0.210 \cdot 0.106 + 0.403 \cdot 0.192 \cdot = 0.456$$

This value falls within the fourth bin of the sub-table PGV = 30 cm/s of Table 4. The following probabilities are predicted: A (usable) = 35.5%, B (partially unusable) = 11.2%, E (unusable) = 53.3%.

If a PGV = 12 cm/s is assumed for the site, the lower category PGV = 10 cm/s needs to be considered and applying again the previous procedure *U* = 0.241 is obtained. This figure falls again within the fourth bin of the sub-table PGV = 10 cm/s

of Table 4. This behavior is systematic: the explanatory building will always fall within the fourth bin of each PGV sub-table.

If the structural class is changed from 4 to 1, the following result is obtained for PGV = 30 cm/s: $U = 0.295$, falling within the second bin of the sub-table PGV = 30 cm/s of Table 4, thus delivering: A = 69.5%, B = 13.8%, E = 16.7%. This comparison highlights the importance of structural class for the seismic performance of a building. However, the proposed model should be used on large building portfolios in order to compensate for statistical errors occurring on individual buildings. Its use on a specific construction can only give a poor estimation of seismic performance, which should be properly assessed by means of structural analysis.

The proposed model delivers usability outcomes given the PGV. If this ground motion intensity measure is not readily available from hazard studies, it can be estimated from spectral ordinates. If site spectra are available, according to Booth (2007), PGV can be evaluated as:

[6] $$\mathrm{PGV} = \frac{\text{peak 5\% damped spectral velocity from smoothed spectrum}}{2.3}$$

Within a code framework the Italian Building Standard (DMIT 2018) estimates PGV as:

[7] $$\mathrm{PGV} = 0.16\, a_g\, S\, T_C$$

where: a_g is the design ground acceleration on stiff and horizontal ground, S is site factor accounting for stratigraphy and topography, T_C is the upper limit of the period of the constant spectral acceleration branch.

Finally, considering that the method proposed is empirical at its core, Table 4 is meant to be used as categorical, as shown in the worked-out example. Nonetheless, interpolation would be possible because of the linear trends present between different intensity measure categories. For the same reason, extrapolation would be possible as well, but bearing in mind that the shakemaps at the base of the proposed model had a maximum PGV of 58 cm/s.

5 CONCLUSIONS

Unreinforced masonry constructions account for a large share of the existing building portfolios in several countries and they are prone to poor seismic performance. Large-scale scenario analyses and preventive mitigation programs need simplified models that streamline survey and computation phases. Several models have been proposed in the past but they are usually focused on vulnerability, i.e. damage proneness, rather than performance such as usability, i.e. the condition of a building being occupiable after a seismic event. Moreover, the formulation of some of these models relies heavily on expert judgment rather than on rigorous analysis of existing databases. Therefore, an empirical model to forecast the usability of existing unreinforced masonry buildings has been recently calibrated based on statistical regressions and principal component analyses of the data of about 60 000 constructions affected by the 2009 L'Aquila earthquake in Italy. This model uses Mercalli-Cancani-Sieberg macroseismic intensity to express ground shaking, the only intensity measure extensively available at the time the model was developed.

The use of empirical models typically saves time and manpower, because very basic data are collected during the survey and no structural analysis is implemented. A limitation of these models is that they are relevant only for the region for which they were calibrated. Therefore, the macroseismic intensity model calibrated on L'Aquila data has been applied here to data collected on 18 000 buildings affected by a 2002 earthquake occurring in another region, Molise, of the same mountain range to which L'Aquila belongs. The comparison between predicted and observed usabilities was fairly encouraging, and the difference between prediction and observation can be related to an approximate estimation of ground

shaking, because a single macroseismic intensity was associated with an entire municipality in 2002, rather than with each settlement or district of a municipality as done in 2009.

Despite such a promising performance, a macroseismic-intensity-based model presents a few shortcomings. Macroseismic intensity is attributed on a conventional basis, according to different scales, and no hazard studies are usually available, especially where seismic catalogs are incomplete. Therefore, it is useful to define innovative models based on ground motion intensity measures, more familiar to practitioners and systematically available from hazard studies. Ground motion intensity measures can be associated with the buildings of the 2009 database by means of recently published shakemaps. Despite their intrinsic approximation, information delivered in a shakemap can be considered at least as robust as macroseismic intensity. Three ground motion parameters have been considered here: peak ground acceleration, peak ground velocity, and spectral pseudoacceleration at a period of vibration of 0.3 s, the most relevant given the features of the constructions considered herein.

For each of these intensity measures, loss-of-usability single-variable regressions have been computed for seven building parameters: building position within the structural aggregate, number of stories above ground, construction timespan, structural class, presence of strengthening interventions, roof type, pre-existing damage to structural elements. Additionally, several principal component analyses have been performed in order to determine relative weights and identify the negligible importance of the number of stories above ground and of the presence of strengthening interventions. The first parameter is relevant only when moving from single-story to multiple-story buildings, but single-story constructions account for a rather limited part of the portfolio and are comparatively newer and better-quality buildings, aspects that are predominant for the prediction of the seismic performance. The presence of strengthening interventions is difficult to detect during a rapid visual inspection and, thus, its impact on the model is not systematic. Of the remaining five parameters, the structural class, a combination of vertical and horizontal structures, is the most relevant.

The usability prediction of the model, for each of the three ground motion parameters considered, has been compared with the usability observation after the 2009 earthquake. The agreement is rather encouraging for all three parameters, with peak ground velocity being the best choice in terms of coefficient of determination with respect to the bisector line of the plane prediction-observation. On the contrary, peak ground acceleration and spectral pseudoacceleration are less effective. Therefore, usability probability matrices are computed only for peak ground velocity, which is frequently available from hazard studies or can be estimated from spectral ordinates. The model is presented with all necessary loss-of-usability coefficients and principal-component-analysis weights, allowing the reader to follow a worked-out example and to independently implement the model for scenario analyses.

The new ground-motion-based model has been calibrated on data from a specific Italian region, but the validation of its previous macroseismic-intensity version with data from a neighboring region is encouraging. Therefore, it may be expected that the model can deliver at least tentative estimations for other Italian regions presenting natural-stone masonry buildings such as can be found along most of the Apennine mountain range and part of the Alpine belt. Similar constructions can be found in other European earthquake prone areas, such as those in the Balkans, Greece, and Portugal: it would be worth carrying out additional validations if building and ground motion data are available. Finally, a natural extension of the model would be to include reinforced-concrete constructions, which in Italy account for a smaller number of buildings but with a larger average volume.

6 ACKNOWLEDGEMENTS

The authors wish to thank the Dipartimento di Protezione Civile for granting access to the damage and usability database of the 2009 L'Aquila earthquake. This work was partially carried out under the programs "Dipartimento della Protezione Civile – Consorzio RELUIS". The opinions expressed in this publication are solely those of the authors and are not necessarily endorsed by the Dipartimento di Protezione Civile.

7 REFERENCES

Abrams DP, AlShawa O, Lourenço PB, Sorrentino L (2017) Out-of-Plane Seismic Response of Unreinforced Masonry Walls: Conceptual Discussion, Research Needs, and Modeling Issues. Int J Archit Herit 11:22–30. doi: 10.1080/15583058.2016.1238977

AlShawa O, Liberatore D, Sorrentino L (2019) Dynamic One-Sided Out-Of-Plane Behavior of Unreinforced-Masonry Wall Restrained by Elasto-Plastic Tie-Rods. Int J Archit Herit. doi: 10.1080/15583058.2018.1563226

Aschheim MA, Black EF, Cuesta I (2002) Theory of principal components analysis and applications to multistory frame buildings responding to seismic excitation. Eng Struct 24:1091–1103. doi: 10.1016/S0141-0296(02)00036-6

ATC-13 (1985) Earthquake Damage Evaluation Data for California. Applied Technology Council, Redwood City, California

Augenti N, Parisi F (2010) Learning from Construction Failures due to the 2009 L'Aquila, Italy, Earthquake. J Perform Constr Facil 24:536–555. doi: 10.1061/(ASCE)CF.1943-5509.0000122

Baggio C, Bernardini A, Colozza R, et al (2007) Field Manual for post-earthquake damage and safety assessment and short term countermeasures (AeDES). European Communities, 2007 Reproduction

Barbat AH, Yépez Moya F, Canas JA (1996) Damage Scenarios Simulation for Seismic Risk Assessment in Urban Zones. Earthq Spectra 12:371–394.

Benedetti D, Petrini V (1984) Sulla vulnerabilita sismica di edifici in muratura: un metodo di valutazione. A method for evaluating the seismic vulnerability of masonry buildings. L'industria delle Costr 19:66–74.

Bertelli S, Rossetto T, Ioannou I (2018) Derivation of Empirical Fragility Functions From the 2009 Aquila Earthquake. In: 16th European Conference on Earthquake Engineering. Thessaloniki, pp 1–12

Booth E (2007) The estimation of peak ground-motion parameters from spectral ordinates. J Earthq Eng 11:13–32. doi: 10.1080/13632460601123156

Borzi B, Pinho R, Crowley H (2008) Simplified pushover-based vulnerability analysis for large-scale assessment of RC buildings. Eng Struct 30:804–820. doi: 10.1016/j.engstruct.2007.05.021

Braga F, Dolce M, Liberatore D (1982) A Statistical Study on Damaged Buildings and an Ensuing Review of the MSK-76 Scale. In: Seventh European Conference on Earthquake Engineering. pp 431–450

Calvi GM, Pinho R, Magenes G, et al (2006) Development of seismic vulnerability assessment methodologies over the past 30 years. ISET J Earthq Technol 43:75–104.

Colonna S, Imperatore S, Zucconi M, Ferracuti B (2017) Post-seismic damage assessment of a historical masonry building: The case study of a school in Teramo. In: International Conference on Mechanics of Masonry Structures Strengthened with Composites Materials, MuRiCo5, Bologna, Italy, 28-30 June. Key Engineering Materials, Bologna, pp 620–627

D'Ayala D (2013) Assessing the seismic vulnerability of masonry buildings. In: Handbook of Seismic Risk Analysis and Management of Civil Infrastructure Systems. pp 334–365

de Leeuw ED, Hox JJ, Dillam DA (2012) International Handbook of Survey Methodology. Routledge

Del Gaudio C, De Martino G, Di Ludovico M, et al (2017) Empirical fragility curves from damage data on RC buildings after the 2009 L'Aquila earthquake. Bull Earthq Eng 15:1425–1450. doi: 10.1007/s10518-016-0026-1

Di Ludovico M, Prota A, Moroni C, et al (2017a) Reconstruction process of damaged residential buildings outside historical centres after the L'Aquila earthquake: part I—"light damage" reconstruction. Bull Earthq Eng 15:667–692. doi: 10.1007/s10518-016-9877-8

Di Ludovico M, Prota A, Moroni C, et al (2017b) Reconstruction process of damaged residential buildings outside historical centres after the L'Aquila earthquake: part II—"heavy damage" reconstruction. Bull Earthq Eng 15:693–729. doi: 10.1007/s10518-016-9979-3

DMIT (2018) Decreto del Ministro delle Infrastrutture e dei Trasporti 17 gennaio 2018. Aggiornamento delle "Norme tecniche per le costruzioni".

Dolce M, Di Bucci D (2014) National Civil Protection Organization and technical activities in the 2012 Emilia earthquakes (Italy). Bull Earthq Eng 12:2231–2253. doi: 10.1007/s10518-014-9597-x

Dolce M, Goretti A (2015) Building damage assessment after the 2009 Abruzzi earthquake. Bull Earthq Eng 13:2241–2264. doi: 10.1007/s10518-015-9723-4

Dolce M, Manfredi G (2015) Libro Bianco Sulla Ricostruzione Privata Fuori Dai Centri Storici Nei Comuni Colpiti Dal Sisma Dell'Abruzzo Del 6 Aprile 2009. Doppiavoce, Napoli

Dolce M, Speranza E, Giordano F, et al (2017) Da . D . O - Uno strumento per la consultazione e la comparazione del danno osservato relativo ai più significativi eventi sismici in Italia dal 1976 . In: XXVII Convegno ANIDIS-L'Ingegneria Sismica in Italia. Pistoia, pp 348–357

EC8-1 (2004) Eurocode 8: Design of structures for earthquake resistance - Part 1: General rules, seismic actions and rules for buildings. European Committee for Standardization, Brussels, Brussels

Erberik MA (2008) Generation of fragility curves for Turkish masonry buildings considering in-plane failure modes. Earthq Eng Struct Dyn Eng 37:387–405. doi: 10.1002/eqe.760

Faenza L, Lauciani V, Michelini A (2011) Rapid determination of the shakemaps for the L'Aquila main shock: a critical analysis. Boll di Geofis Teor ed Appl 52:407–425. doi: 10.4430/bgta0020

Fajfar P (2000) A nonlinear analysis method for Performance-based Seismic Design. Earthq Spectra 16:573–592.

Ferlito R, Guarascio M, Zucconi M (2013) Assessment of a vulnerability model against post-earthquake damage data: The case study of the historic city centre of L'Aquila in Italy. In: 9th World Conference on Earthquake Resistant Engineering Structures, A Coruna, Spain, 8-10 July. WIT Transactions on the Built Environment, pp 393–404

Formisano A, Florio G, Landolfo R, Mazzolani FM (2011) Numerical Calibration of a Simplified Procedure for the

Seismic Behaviour Assessment of Masonry Building Aggregates. 13th Int Conf Civil, Struct Environ Eng Comput Stirlingshire, Scotl 1–28. doi: http://dx.doi.org/10.1016/j.advengsoft.2014.09.013

Galli P, Camassi R, Azzaro R, et al (2009) Il Terremoto Aquilano del 6 Aprile 2009: Rilievo Macrosismico, Effetti di Superficie ed Implicazioni Sismotettoniche. Quat Ital J Quat Sci 22:235–246.

Gebelein J, Barnard M, Burton H, et al (2017) Considerations for a Framework of Resilient Structural Design for Earthquakes. In: 2017 Seaoc Convention Proceedings. pp 1–16

Giuffrè A (1996) A mechanical model for statics and dynamics of historical masonry buildings. In: Petrini V, Save M (eds) Protection of the Architectural Heritage Against Earthquakes. Springer, Wien, pp 71–153

Goretti A, Di Pasquale G (2004) Building inspection and damage data for the 2002 Molise, Italy, earthquake. Earthq Spectra 20:S167–S190. doi: 10.1193/1.1769373

Grünthal G (1998) Cahiers du Centre Européen de Géodynamique et de Séismologie: Volume 15 – European Macroseismic Scale 1998. European Center for Geodynamics and Seismology, Luxembourg

Gutiérrez E, Zaldivar JM (2000) The application of Karhunen-Loeve, or principal component analysis method, to study the non-linear seismic response of structures. Earthq Eng Struct Dyn 29:1261–1286. doi: 10.1002/1096-9845(200009)29:9<1261::AID-EQE964>3.0.CO;2-N

Jolliffe IT (2002) Principal Component Analysis, Second Edition, 2nd edn. New York

Kappos AJ, Panagopoulos G, Panagiotopoulos C, Penelis G (2006) A hybrid method for the vulnerability assessment of R/C and URM buildings. Bull Earthq Eng 4:391–413. doi: 10.1007/s10518-006-9023-0

L (1962) Legge 1684. Provvedimenti per l'edilizia con particolari prescrizioni per le zone sismiche. Gazzetta Ufficiale della Repubblica Italiana, 22 dicembre 1962, n. 326

Lagomarsino S, Giovinazzi S (2006) Macroseismic and mechanical models for the vulnerability and damage assessment of current buildings. Bull Earthq Eng 4:415–443. doi: 10.1007/s10518-006-9024-z

Locati M, Camassi R, Rovida A, et al (2016) DBMI15, the 2015 version of the Italian Macroseismic Database.

Loh CH, Chan CK, Chen SF, Huang SK (2016) Vibration-based damage assessment of steel structure using global and local response measurements. 45:699–718. doi: 10.1002/eqe.2680

Magenes G, Penna A, Senaldi IE, et al (2014) Shaking table test of a strengthened full-scale stone masonry building with flexible diaphragms. Int J Archit Herit 8:349–375. doi: 10.1080/15583058.2013.826299

Massumi A, Gholami F (2016) The influence of seismic intensity parameters on structural damage of RC buildings using principal components analysis. 40:2161–2176. doi: 10.1016/j.apm.2015.09.043

MathWorks (2016) Matlab.

Mouyiannou A, Penna A, Rota M, et al (2014) Implications of cumulated seismic damage on the seismic performance of unreinforced masonry buildings. Bull New Zeal Soc Earthq Eng 47:157–170.

Musson RMW, Grünthal G, Stucchi M (2010) The comparison of macroseismic intensity scales. J Seismol 14:413–428. doi: 10.1007/s10950-009-9172-0

Ni YQ, Zhou XT, Ko JM (2006) Experimental investigation of seismic damage identification using PCA-compressed frequency response functions and neural networks. 290:242–263. doi: 10.1016/j.jsv.2005.03.016

Pinto A, Taucer F (2007) Field Manual for post-earthquake damage and safety assessment and short term countermeasures

(AeDES). European Commission, Joint Research Centre, Institute for the Protection and Security of the Citizen, Ispra

Ramos LF, Lourenço PB (2004) Modeling and vulnerability of historical city centers in seismic areas: a case study in Lisbon. Eng Struct 26:1295–1310. doi: 10.1016/j.engstruct.2004.04.008

Rossetto T, D'Ayala D, Gori F, et al (2014) The value of multiple earthquake missions: The EEFIT L'Aquila earthquake experience. Bull Earthq Eng 12:277–305. doi: 10.1007/s10518-014-9588-y

Rosti A, Rota M, Penna A (2018) Damage classification and derivation of damage probability matrices from L'Aquila (2009) post-earthquake survey data. Bull Earthq Eng 16:3687–3720. doi: 10.1007/s10518-018-0352-6

Rota M, Penna A, Strobbia C, Magenes G (2011) Typological seismic risk maps for Italy. Earthq Spectra 27:907–926. doi: 10.1193/1.3609850

Rota M, Penna A, Strobbia CL (2008) Processing Italian damage data to derive typological fragility curves. Soil Dyn Earthq Eng 28:933–947. doi: 10.1016/j.soildyn.2007.10.010

Sisti R, Di Ludovico M, Borri A, Prota A (2018) Damage assessment and the effectiveness of prevention: the response of ordinary unreinforced masonry buildings in Norcia during the Central Italy 2016–2017 seismic sequence. Bull Earthq Eng 1–21. doi: 10.1007/s10518-018-0448-z

Sorrentino L (2007) The early entrance of dynamics in earthquake engineering: Arturo Danusso's contribution. ISET J Earthq Technol 44:1–24.

Sorrentino L, Bruccoleri D, Antonini M (2008) Structural interpretation of post-earthquake (19th century) retrofitting on the Santa Maria degli Angeli Basilica, Assisi, Italy. In: Sixth International Conference on Structural Analysis of Historic Construction, 2-4 July, Bath. pp 217–225

Sorrentino L, Cattari S, Da Porto F, et al (2018) Seismic behaviour of ordinary masonry buildings during the 2016 Central Italy Earthquake. Bull Earthq Eng. doi: 10.1007/s10518-018-0370-4.

Sorrentino L, Tocci C (2008) The structural strengthening of early and mid 20th century reinforced concrete diaphragms. In: Sixth International Conference on Structural Analysis of Historic Construction, 2-4 July, Bath. pp 1431–1439

Spence R, Coburn AW, Pomonis A (1992) Correlation of Ground Motion with Building Damage: The Definition of a New Damage-Based Seismic Intensity Scale. In: 10th World Conference on Earthquake Engineering. Madrid, Spain, pp 551–556

Stannard M, Galloway B, Brunsdon D, et al (2014) Field Guide: Rapid Post Disaster Building Usability Assessment - Earthquakes. Ministry of Business, Innovation and Employment, Wellington, New Zealand

Vicente R, Parodi S, Lagomarsino S, et al (2011) Seismic vulnerability and risk assessment: Case study of the historic city centre of Coimbra, Portugal. Bull Earthq Eng 9:1067–1096. doi: 10.1007/s10518-010-9233-3

Walsh KQ, Cummuskey PA, Jafarzadeh R, Ingham JM (2017) Rapid Identification and Taxonomical Classification of Structural Seismic Attributes in a Regionwide Commercial Building Stock. J Perform Constr Facil 31:04016067. doi: https://doi.org/10.1061/(ASCE)CF.1943-5509.0000927

Whitman RV, Reed JW, Hong ST (1973) Earthquake Damage Probability Matrices. In: 5th World Conference on Earthquake Engineering. Rome, pp 2531–2540

Zuccaro G, Cacace F (2015) Seismic vulnerability assessment based on typological characteristics. The first level

procedure “SAVE.” Soil Dyn Earthq Eng 69:262–269. doi: 10.1016/j.soildyn.2014.11.003

Zucconi M, Ferlito R, Sorrentino L (2018a) Simplified survey form of unreinforced masonry buildings calibrated on data from the 2009 L’Aquila earthquake. Bull Earthq Eng 16:2877–2911. doi: 10.1007/s10518-017-0283-7

Zucconi M, Ferlito R, Sorrentino L (2018b) Verification of a usability model for unreinforced masonry buildings with data from the 2002 Molise, Earthquake. In: Proceedings of the International Masonry Society Conferences (ed) 10th International Masonry Conference, IMC, Milan, Italy, 9-11 July. Milano, pp 680–688

Zucconi M, Sorrentino L, Ferlito R (2017) Principal component analysis for a seismic usability model of unreinforced masonry buildings. Soil Dyn Earthq Eng 96:64–75. doi: 10.1016/j.soildyn.2017.02.014

APPENDIX A. LOSS-OF-USABILITY COEFFICIENTS

In order to make the new ground-motion-intensity-measure model fully applicable, the loss-of-usability coefficients associated with the five building parameters relevant for seismic performance are presented in the following tables for the PGV categories of Table 2.

Category	PGV [cm/s]				
	2.5	10	20	30	45
Isolated	0.060	0.115	0.183	0.251	0.353
Internal	0.128	0.212	0.318	0.423	0.582
End of row	0.121	0.187	0.270	0.353	0.478
Corner	0.131	0.224	0.340	0.456	0.629

Table A.1. Loss-of-usability coefficients u_i (Eq. [1]) for position within the structural aggregate parameter.

Category	PGV [cm/s]				
	2.5	10	20	30	45
< 1919	0.153	0.245	0.361	0.476	0.648
1919 - 1945	0.086	0.178	0.293	0.408	0.580
1946 - 1961	0.049	0.116	0.199	0.282	0.407
>1961	0.017	0.051	0.092	0.134	0.196

Table A.2. Loss-of-usability coefficients u_i (Eq. [1]) for construction timespan parameter.

Category	PGV [cm/s]				
	2.5	10	20	30	45
Structural class 1	0.010	0.043	0.084	0.125	0.187
Structural class 2	0.061	0.111	0.174	0.237	0.332
Structural class 3	0.067	0.146	0.245	0.344	0.492
Structural class 4	0.183	0.286	0.414	0.542	0.735

Table A.3. Loss-of-usability coefficients u_i (Eq. [1]) for structural class parameter. Structural classes are defined in Table 1.

Category	PGV [cm/s]				
	2.5	10	20	30	45
Thrusting heavy	0.092	0.161	0.247	0.333	0.463
Non thrusting heavy	0.043	0.091	0.151	0.210	0.300
Thrusting light	0.163	0.252	0.364	0.476	0.643
Non thrusting light	0.134	0.209	0.301	0.394	0.533

Table A.4. Loss-of-usability coefficients u_i (Eq. [1]) for roof type parameter.

Category	PGV [cm/s]				
	2.5	10	20	30	45
D0	0.073	0.144	0.231	0.319	0.450
D1	0.175	0.240	0.321	0.403	0.525
D2	0.386	0.470	0.574	0.678	0.835
D3	0.431	0.513	0.614	0.716	0.869
D4	0.468	0.559	0.672	0.785	0.955

Table A.5. Loss-of-usability coefficients u_i (Eq. [1]) for pre-existing structural damage parameter.